ORGANOMETALLICS
Article
Cite This: Organometallics 2018, 37, 4195−4203
pubs.acs.org/Organometallics

Why Two Metals Are Better Than One for Heterodinuclear Cobalt−Zirconium-Catalyzed Kumada Coupling

Jimmy Coombs,[†] Dalton Perry,[†] Doo-Hyun Kwon,[†] Christine M. Thomas,[‡] and Daniel H. Ess*[,†]

[†]Department of Chemistry and Biochemistry, Brigham Young University, Provo, Utah 84602, United States
[‡]Department of Chemistry and Biochemistry, The Ohio State University, Columbus, Ohio 43210, United States

Supporting Information

ABSTRACT: Heterodinuclear transition metal complexes with a direct metal−metal interaction offer the potential of unique reactivity compared with mononuclear catalysts. Heterodinuclear Co−Zr complexes with phosphinoamide ligands bridging Co and Zr metal centers are effective precatalysts for Kumada C−C bond coupling reactions between alkyl halides and alkyl Grignards. In contrast, the analogous mononuclear Co tris(phosphinoamine) complex without Zr provides very inefficient catalysis. Here we describe density functional theory calculations that reveal the mechanistic and reactivity impact of the Co−Zr metal−metal interaction and phosphinoamide ligands on alkyl halide−alkyl Grignard Kumada coupling catalysis. The Co−Zr interaction enables two-electron reduction of the precatalyst to form an active catalyst, which then promotes a low-energy electron-transfer alkyl halide oxidative addition mechanism. The Co−Zr interaction and the phosphinoamide ligands bridging the metal centers provide a dialkyl intermediate with a low-energy C−C bond forming reductive elimination route through a phosphine dissociation pathway, which is not viable for an analogous mononuclear Co complex.

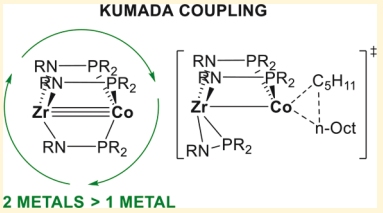

INTRODUCTION

Heterodinuclear transition metal catalysts with a direct covalent or dative/electrostatic metal−metal interaction offer the potential of unique reactivity and selectivity that may not be available to similar mononuclear catalysts.[1] During the 1980s and 1990s, a few heterodinuclear catalysts were reported for a limited set of reactions, such as alkene and ketone hydrogenation,[2] α-olefin hydroformylation,[3] ethylene polymerization,[4] and olefin metathesis.[5] Recently, there has been a major surge in the synthesis of nonbiological heterodinuclear transition metal complexes intended for catalytic application toward challenging transformations,[6−8] for example, arene C−H borylation,[9] carbon dioxide hydrogenation,[10] and dinitrogen reduction.[11]

Early theoretical studies examined heterodinuclear metal−metal bonding, but only a few recent studies have examined heterodinuclear catalysis.[11,12] In most cases, the mechanisms and origin of the unique reactivity and selectivity for heterodinuclear catalysts, especially compared to mononuclear catalysts, remain unknown, which hinders new catalyst development. Our group uses density functional theory (DFT) calculations to identify mechanisms and discover the origin of the unique reactivity and selectivity of heterodinuclear catalysts. For example, we previously identified the mechanism and origin of reactivity and selectivity for heterodinuclear Pd−Ti−phosphinoamide-catalyzed allylic amination[13] and Ir−Ta-catalyzed alkene hydrogenation (Scheme 1a).[14] For the Pd−Ti case, our calculations revealed that because of the unique phosphinoamide ligand scaffold a weak heterodinuclear metal−metal interaction in the ground state can be enhanced in the transition state leading to relatively fast catalysis.[13] This discovery prompted us to examine the unique Kumada coupling reactivity catalyzed by heterodinuclear Co−Zr complexes bearing similar phosphinoamide ligands.

Scheme 1. (a) Examples of Heterodinuclear Catalysts We Previously Examined using DFT Calculations and (b) Co−Zr Heterodinuclear Catalysis Examined in This Work

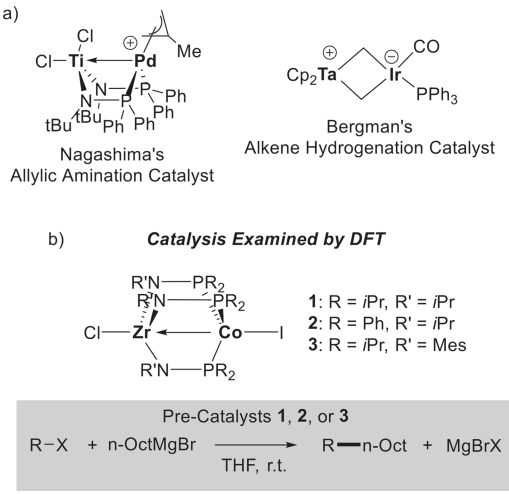

In 2011, Thomas reported the Kumada C−C bond coupling reaction between alkyl halides and alkyl Grignards catalyzed by a series of heterodinuclear precatalyst Co−Zr complexes (Scheme 1b).[15,16] Precatalysts **1**−**3** [(ClZr(R′NPR$_2$)$_3$CoI)] (R = *i*Pr or

Received: June 30, 2018
Published: November 8, 2018

DOI: 10.1021/acs.organomet.8b00449
Organometallics 2018, 37, 4195−4203

Ph; R′ = *i*Pr or Mes) feature phosphinoamide ligands bridging Co and Zr metal centers with a direct metal−metal interaction. These heterodinuclear precatalysts generally gave moderate to high yields of C−C bond coupling alkane products. For example, the use of 5 mol % precatalyst **1** with 30 mol % TMEDA in THF at room temperature led to yields generally between 60 and 99% for coupling between primary and secondary alkyl halides and *n*-OctMgBr. Importantly, while Kumada couplings are often catalyzed by mononuclear catalysts,[17] sp^3−sp^3 couplings are rarely catalyzed by mononuclear Co complexes,[18] and the analogous mononuclear Co tris(phosphinoamine) complex does not provide efficient catalysis with only trace alkane product yields for reaction between alkyl halides and *n*-OctMgBr.[15] This very different reactivity of the dinuclear Co−Zr catalysts versus the mononuclear Co complex further stimulated our interest in identifying an operating mechanism and the origin of the unique dinuclear reactivity.

Here we report DFT calculations that examine the mechanistic and reactivity impact of the Co−Zr metal−metal interaction, and phosphinoamide ligands, on Kumada sp^3−sp^3 coupling catalysis. We discovered that the Co−Zr interaction enables two-electron reduction of the precatalyst to form an active catalyst, and this active catalyst promotes a low-energy electron-transfer-induced alkyl halide oxidative addition mechanism. Furthermore, the Co−Zr interaction and phosphinoamide ligands also provide a dialkyl intermediate with a low-energy C−C bond-forming reductive elimination pathway that involves phosphine dissociation. Together, these effects provide a unique mechanism and efficient catalysis not available to mononuclear Co analogues.

RESULTS AND DISCUSSION

Precatalyst and Catalyst Structures. We decided to examine Kumada precatalyst **1** because it induced the largest coupling yields.[15] Under reducing Grignard conditions, precatalyst **1** is likely transformed into an active catalytic species. Thomas observed that chemical two-electron reduction of complex **3** in THF resulted in the formation of the (THF)Zr(MesNP*i*Pr$_2$)$_3$Co(N$_2$) complex (Scheme 2a).[15] Reaction of this complex with alkyl halides resulted in the observation of oxidized intermediates. This prompted us to explore the thermodynamics for precatalyst activation of **1** by one- and two-electron transfer (ET) and halide ligand loss. We modeled the Grignard species as a dinuclear bridged [(*n*-Oct)MgBr]$_2$ structure (Scheme 2b), which has been our model for other Grignard-type reactions.[19] ET between this Grignard model and precatalyst **1** requires >40 kcal/mol and is unlikely. Dissociation of phosphine from the Co metal center does not substantially reduce the thermodynamic requirement for ET from the Grignard to the Co−Zr complex. Instead, the most likely precatalyst activation pathway involves iodide dissociation followed by ET, which may occur in one step. The resulting reduced Cl−Zr(*i*PrNP*i*Pr$_2$)$_3$Co structure **4** (Scheme 2b) is a viable intermediate with a ΔG of −3.2 kcal/mol. A second ET is possible after or at the same time as chloride dissociation, which results in the doubly reduced Co−Zr intermediate **5** that is similar to the structure that was observed experimentally through Na/Hg reduction. **5** is endergonic by 15.6 kcal/mol, but overall, this precatalyst activation is thermodynamically favorable considering formation of hexadecane (C$_{16}$H$_{34}$) along with MgBr$_2$ and MgICl is exergonic by 61.6 kcal/mol.

Because of the thermodynamic viability of **4** and **5**, these were the major heterodinuclear catalytic structures examined for the coupling between 1-bromopentane (C$_5$H$_{11}$Br) and *n*-OctMgBr. We also examined catalyst **5** with an explicit THF coordinated to the Zr metal center. However, weakly coordinated THF did not significantly impact structures and energies (see the Supporting Information). For mononuclear ICo(*i*Pr$_2$PNH*i*Pr)$_3$ complex **6** (Scheme 2b), which has related phosphinoamine ligands compared to the phosphinoamide ligands of **1**, we examined catalysis from the one-electron-reduced version **7** as well as the corresponding anionic two-electron reduced complex.

Scheme 2. (a) Chemical Reduction of Co−Zr Complex 3 Reported by Thomas[15] and (b) Dinuclear Grignard, Co−Zr Dinuclear, and Co Mononuclear Catalyst Models

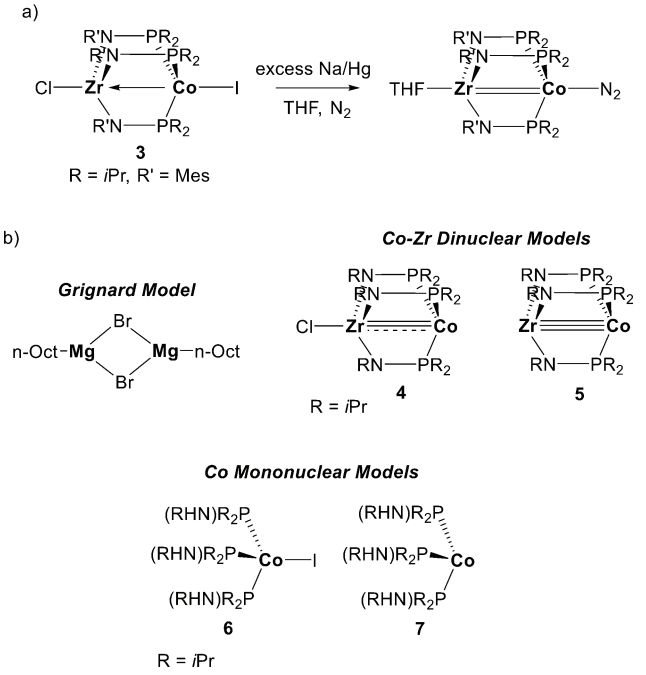

Figure 1 displays the M06-L DFT molecular orbitals that describe the major Co−Zr interactions in **5**. As expected, HOMO−4 (orbital 156), HOMO−3 (orbital 157), and HOMO−2 (orbital 158) represent the σ and degenerate π orbitals for the Co−Zr triple-bond character.[15,16] Occupied orbitals 159 and 160 (degenerate HOMO and HOMO−1) are Co-centered nonbonding electron pairs. The LUMO is Co−Zr σ^* orbital 161. We initially assumed that **5** would have multireference character and be best described as a mixture of electronic configurations. However, we found the triplet spin state to be 18.1 kcal/mol higher in energy, which suggests a relatively large HOMO−LUMO gap and a lack of multireference character. Indeed, the HOMO−LUMO gap is relatively large at 2.1 eV. Attempted reoptimization of the M06-L wave function with a broken symmetry guess using unrestricted orbitals did not lead to a lower-energy singlet wave function, which suggests a dominant single-reference description.

Oxidative Addition and Transmetalation. Most cross-coupling reactions between alkyl halides and Grignards catalyzed by mononuclear Ni, Pd, and Cu complexes have been proposed to proceed via closed-shell two-electron mechanisms, which involve the typical three steps of oxidation addition, transmetalation, and reductive elimination.[20] In contrast, for a few mononuclear Co-catalyzed coupling reactions, typically between alkyl halides and aryl or allylic

DOI: 10.1021/acs.organomet.8b00449
Organometallics 2018, 37, 4195−4203

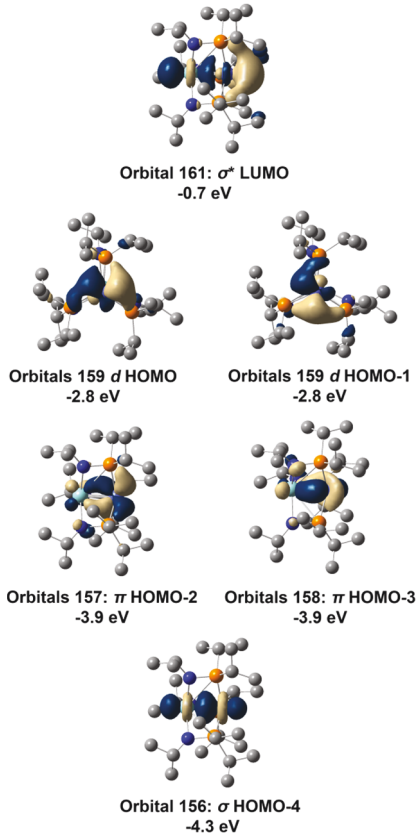

Figure 1. M06-L closed-shell orbitals for catalyst **5** showcasing σ (HOMO−4) and π orbitals (HOMO−2 and HOMO−3) of the Co−Zr interaction. Color coding: gray, carbon; blue, nitrogen; orange, phosphorus; purple, cobalt; light blue, zirconium. Hydrogen atoms have been omitted.

Grignards, open-shell mechanisms have been proposed.[21] Because catalyst **5** is a low-spin closed-shell complex, for oxidative addition with 1-bromopentane we examined both closed-shell and open-shell mechanisms.

Oxidative addition at the Co metal center between **5** and 1-bromopentane to give $[Zr(i\text{PrNP}i\text{Pr}_2)_3Co(C_5H_{11})(Br)]$ **8** is endergonic with a ΔG of 11.8 kcal/mol (Scheme 3a). We were surprised to find that a one-step oxidative addition transition state to give **8** with a distorted square pyramidal Co metal center requires a $\Delta G^{\ddagger}$ of >40 kcal/mol. The alternative oxidation addition with addition across both metal centers gives $[(Br)Zr(i\text{PrNP}i\text{Pr}_2)_3Co(C_5H_{11})]$ (ΔG = 4.5 kcal/mol) and $[(C_5H_{11})Zr(i\text{PrNP}i\text{Pr}_2)_3Co(Br)]$ (ΔG = 0.2 kcal/mol). While these complexes are slightly lower in energy than **8**, a low-energy one-step pathway for dinuclear oxidative addition is unlikely because the HOMO and HOMO−1 orbitals of **5** are localized only on the Co metal center and HOMO−2 and HOMO−3 orbitals have π-type symmetry (see the Supporting Information for analysis of one-step pathways).

Without a one-step oxidative addition pathway available, we examined the plausible multistep nucleophilic substitution and ET-type pathways. The $\Delta G^{\ddagger}$ for nucleophilic substitution of bromide with Co is 24.6 kcal/mol and results in the ion pair $[Zr(i\text{PrNP}i\text{Pr}_2)_3Co(C_5H_{11})]^+[Br]^-$ with a ΔG of 6.2 kcal/mol. For the separated ions, $[Zr(i\text{PrNP}i\text{Pr}_2)_3Co(C_5H_{11})]^+$ **10** and bromide, ΔG = 13.0 kcal/mol. ET from **5** to 1-bromopentane was the lowest-energy pathway identified[22] and requires a ΔG of 8.5 kcal/mol to give the radical cation Co−Zr intermediate **9** and $(C_5H_{11}Br)^{*-}$ (* = unpaired electron), which has a nearly severed C−Br bond. After ET, a potential energy surface scan showed no potential energy barrier for the combination of **9** and the pentyl radical to give cationic intermediate **10**, and coordination of bromide provides a route to oxidative addition intermediate **8**. $[(Br)Zr(i\text{PrNP}i\text{Pr}_2)_3Co(C_5H_{11})]$ or $[(C_5H_{11})$-$Zr(i\text{PrNP}i\text{Pr}_2)_3Co(Br)]$ complexes could also be produced from **9**, but to complete a viable catalytic cycle would require isomerization to **8** or a later catalytic intermediate (see the discussion below and the Supporting Information). Interestingly, while ET occurs from a Co-centered orbital, after two-

Scheme 3. (a) Outline of Intermediates Involved in Closed-Shell and Open-Shell Oxidative Addition between 5 and 1-Bromopentane,[a] (b) Representative Example of Alternative, but Not Viable, ET Pathways, and (c) Transmetalation between 8 and the Grignard Complex

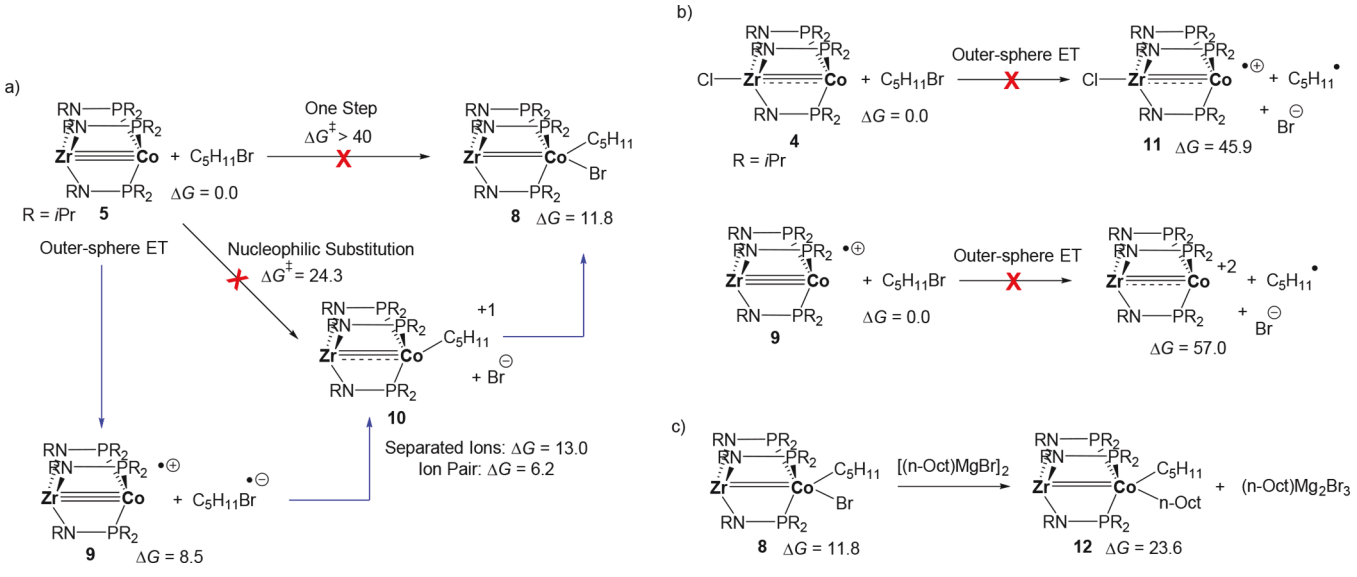

[a]Blue arrows represent the lowest-energy ET pathway identified (values in kilocalories per mole).

DOI: 10.1021/acs.organomet.8b00449
Organometallics 2018, 37, 4195−4203

Scheme 4. (a) Reductive Elimination Transition-State Structure for 12,[a] (b) Reductive Elimination Transition-State Structure for 14,[b] and (c) an Outline ET-Induced Oxidative Addition and Phosphine Dissociation-Induced Reductive Elimination Catalytic Cycle[c]

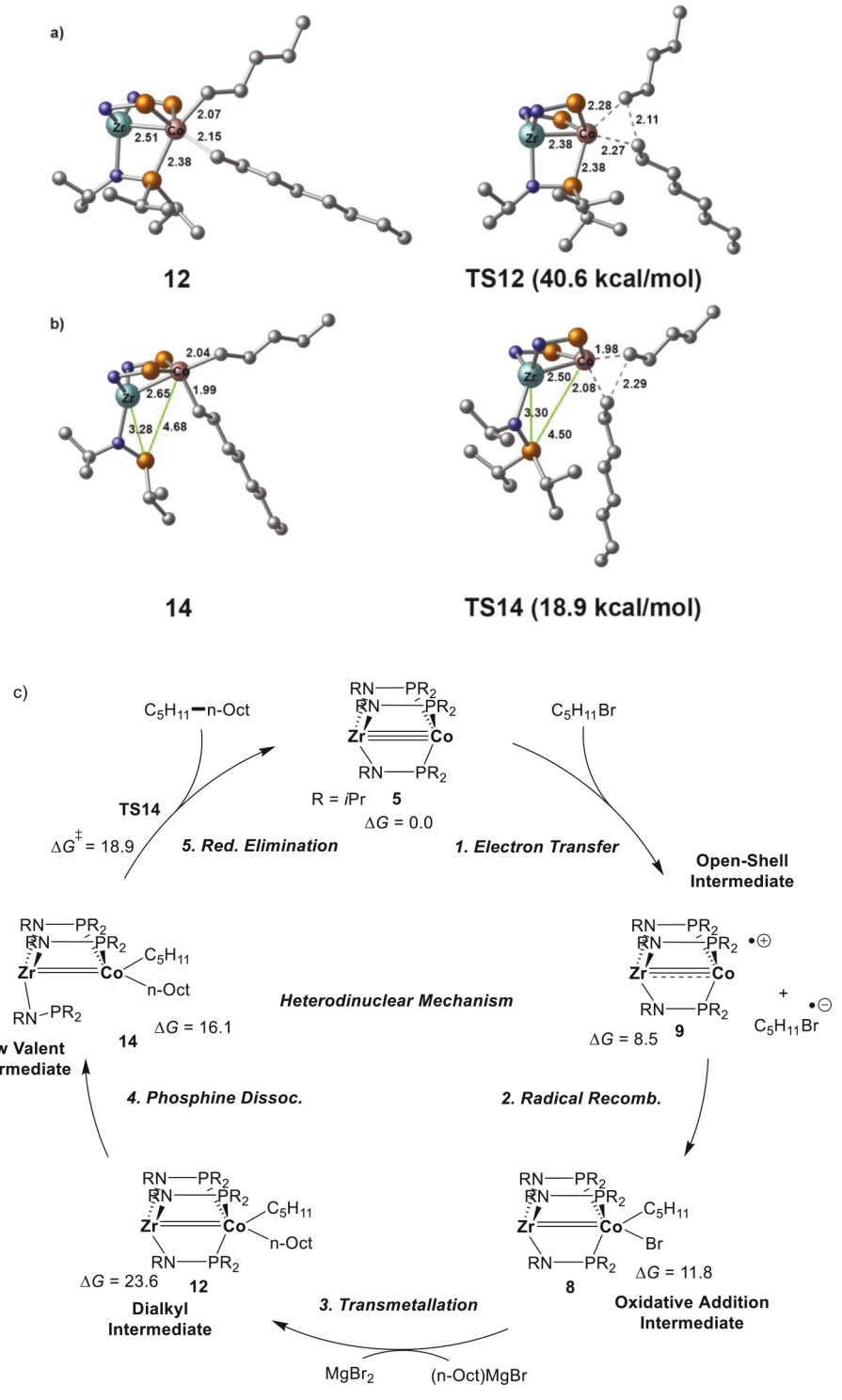

[a]Select *i*Pr groups and all hydrogen atoms have been omitted from the three-dimensional representation. Distances in angstroms. [b]Select *i*Pr groups and all hydrogen atoms have been omitted from the three-dimensional representation. Distances in angstroms. [c]Values in kilocalories per mole.

electron oxidation, inspection of the molecular orbitals indicates that electrons rearrange so that in **8** there is one σ and one π orbital for the Co−Zr interaction.

Our calculations suggesting that catalysis begins with an open-shell ET mechanism for oxidative addition are consistent with multiple experimental observations by Thomas. The most compelling is that addition of TEMPO to a catalytic reaction resulted in the gas chromatography−mass spectrometry observation of both cross-coupling and TEMPO−alkyl products.[15] Interestingly, reaction of 1-bromohexene with

DOI: 10.1021/acs.organomet.8b00449
Organometallics 2018, 37, 4195−4203

(THF)Zr(MesNP*i*Pr$_2$)$_3$Co(N$_2$) resulted in formation of 1-methylcyclopentane, but under catalytic conditions, only C−C coupling products were produced, presumably because coupling is faster than radical cyclization.[15]

There is some evidence of a few previously reported open-shell Kumada coupling mechanisms. On the basis of electron spin resonance, Kochi suggested that a Ni-catalyzed coupling reaction involves open-shell intermediates.[23] More recently, a radical Kumada coupling mechanism involving an Fe^{II} bis-(oxazolinylphenyl)amido pincer complex was proposed by Wodrich and Hu and supported by computational studies.[24] This proposal was based on coupling of enantiomerically enriched substrates that gave a racemic mixture of coupling products and coupling with a cyclopropyl substrate that gave a ring-opened product. On the basis of Mössbauer and DFT calculations, Neidig has also proposed an open-shell mechanism for Kumada coupling with Fe^{II}/Fe^{III}.[25] For related Co-catalyzed alkyl halide−Grignard reactions, Yorimitsu and Oshima reported that isomerization and styrylation reactions with cyclopropylmethyl bromide and 6-bromo-1-hexene substrates provide evidence supporting a radical mechanism.[21c] More recently, Guérinot and Cossy used a radical-clock substrate that resulted in cyclization, presumably through an alkyl radical intermediate.[21e]

Our proposed ET oxidative addition mechanism moderated by catalyst **5** is different from the Fe and Ni monometallic mechanisms proposed by Wodrich and Hu.[24] In the Fe and Ni cases, the Grignard phenyl anion from PhMgBr is proposed to add to the metal center to stimulate electron transfer to an alkyl halide. For **5**, addition of an *n*-Oct anion from the Grignard likely increases the ET capability of this complex, but because **5** is already very rich in electrons, achieving [Zr(*i*PrNP*i*Pr$_2$)$_3$Co(*n*-Oct)]$^-$ is unlikely to be thermodynamically viable. This relatively large thermodynamic penalty to achieve a significantly more electron rich species suggests that **5** is the more likely electron donor. We also examined ET pathways that circumvent intermediate **9**. For example, it is conceivable that [(*n*-Oct)MgBr]$_2$ directly reduces 1-bromopentane to pentyl radical and bromide prior to Co−Zr involvement. However, this is unlikely because the ΔG for 1-bromopentane + [(*n*-Oct)MgBr]$_2$ → (C$_5$H$_{11}$)* + Br$^-$ + ([(*n*-Oct)MgBr]$_2$)*$^+$ is endothermic by 56.2 kcal/mol. Additionally, there are no significant C−C coupling products observed experimentally in the absence of the Co−Zr catalyst. We also explored the possibility that the one-electron-reduced complexes [(Cl)Zr(*i*PrNP*i*Pr$_2$)$_3$Co]* (**4**) and [Zr(*i*PrNP*i*Pr$_2$)$_3$Co]*$^+$ (**9**) could reduce 1-bromopentane (Scheme 3b). For the (Cl)Zr−Co complex, ΔG = 45.9 kcal/mol for **4** + 1-bromopentane → [(Cl)Zr(*i*PrNP*i*Pr$_2$)$_3$Co]$^+$ (**11**) + (C$_5$H$_{11}$)* + Br$^-$. For **9** + 1-bromopentane → [Zr(*i*PrNP*i*Pr$_2$)$_3$Co]$^{2+}$ + (C$_5$H$_{11}$)* + Br$^-$, the ΔG = 57.0 kcal/mol, and this reaction is therefore also unlikely.

After identifying an ET mechanism for achieving oxidized intermediate **8**, we examined the thermodynamics for transmetalation resulting in alkyl/bromide swapping between Co and Mg metal centers (Scheme 3c). For transmetalation between intermediate **8** and [(*n*-Oct)MgBr]$_2$ that results in Zr(*i*PrNP*i*Pr$_2$)$_3$Co(C$_5$H$_{11}$)(*n*-Oct) (**12**), the ΔG for this reaction step is 11.8 kcal/mol, and this added to the 11.8 kcal/mol to achieve **8** results in **12** being endergonic by 23.6 kcal/mol relative to the starting Co−Zr catalyst **5**. While we extensively explored the potential transition-state structures, we could not locate a one-step transmetalation saddle point. Therefore, because this reaction step is endergonic, we have taken the energy of **12** as a low-end estimate of the kinetic barrier for alkyl/bromide group swapping. We also examined possible radical and polar initiated transmetalation pathways, but these pathways were all much higher than the thermodynamics for direct group exchange (see the Supporting Information). As an alternative to transmetalation, we also examined the possibility that [(*n*-Oct)MgBr]$_2$ provides a nucleophilic *n*-Oct anion that directly forms the C−C bond coupling product with simultaneous two-electron metal reduction of either **8** or **10**. However, these pathways are unlikely because the barriers (>39 kcal/mol) are larger than the thermodynamic energy change of transmetalation.

Reductive Elimination and the Catalytic Cycle. Because the Co−Zr metal−metal interaction creates a relatively electron deficient Co metal center, we initially assumed that Zr(*i*PrNP*i*Pr$_2$)$_3$Co(C$_5$H$_{11}$)(*n*-Oct) **12** would be a primed intermediate for facile C−C bond coupling through a one-step, three-center reductive elimination transition state (Scheme 4a, **TS12**). The Co−Zr distance of 2.51 Å in **12** decreases to 2.38 Å in **TS12**, signaling an enhanced metal−metal interaction. However, the $\Delta G^{\ddagger}$ for **TS12** is 40.6 kcal/mol, which is inconsistent with a fast room-temperature reaction. Upon finding this large reductive elimination barrier, we then extensively explored alternative closed-shell and open-shell reductive elimination pathways. For example, we examined Co−alkyl radical fragmentation, which for **12** requires a homolysis bond enthalpy of 17.4 kcal/mol. C−C bond formation could then occur through carbon radical attack of the remaining Co−alkyl bond. The $\Delta G^{\ddagger}$ for this radical C−C bond-forming process is 12.8 kcal/mol. While this could suggest a mixture of tridecane and hexadecane C−C-coupled products, assuming complete radical dissociation into solvent, these products were not reported.[15] We also explored the possibility that the relatively electron rich intermediate **12** could act as an electron donor toward 1-bromopentane. For the donation of electrons from **12** to 1-bromopentane, ΔG = 22.8 kcal/mol to form [Zr(*i*PrNP*i*Pr$_2$)$_3$Co(C$_5$H$_{11}$)(*n*-Oct)]*$^+$ (**13**), (C$_5$H$_{11}$)*, and Br$^-$. Reductive elimination from **13** has a $\Delta G^{\ddagger}$ of 6.6 kcal/mol. While this is a relatively low-energy ET/reductive elimination pathway, we identified a lower-energy reductive elimination pathway that involves phosphine dissociation outlined in panels b and c of Scheme 4.

The Zr metal center plays multiple roles to facilitate reductive elimination. More important than the Co−Zr interaction that creates a relatively electron deficient Co metal center, phosphine dissociation to create an even more electron deficient and low-coordinate Co metal center prepared for reductive elimination is possible because the amido group remains linked to the Zr metal center.[26] This intramolecular dissociation is favorable relative to **12** by 7.5 kcal/mol. In the phosphine dissociation intermediate, **14** (Scheme 4b), the Co−P length increases to 4.68 Å from 2.38 Å in **12** and there is essentially no interaction between the phosphine and the Co metal center. The Co metal center adopts a trigonal bipyramidal geometry with the *n*-Oct group oriented closer to the Zr metal center. There is a weak interaction between the dislodged phosphine and the Zr metal center demonstrated by a distance of 3.28 Å. Phosphine dissociation, by providing a less electron rich and low-coordinate Co metal center, results in a dramatically lower-energy pathway for a one-step reductive elimination transition state, **TS14** (Scheme 4b). The $\Delta G^{\ddagger}$ for **TS14** is only 2.8 kcal/mol relative to intermediate **14** and 18.9 kcal/mol relative to intermediate **5**. This low-energy pathway for C−C bond coupling contrasts with the potentially

DOI: 10.1021/acs.organomet.8b00449
Organometallics 2018, 37, 4195−4203

Scheme 5. Outline of the Mononuclear Structures and Energies for Comparison to the Dinuclear Catalytic Cycle[a]

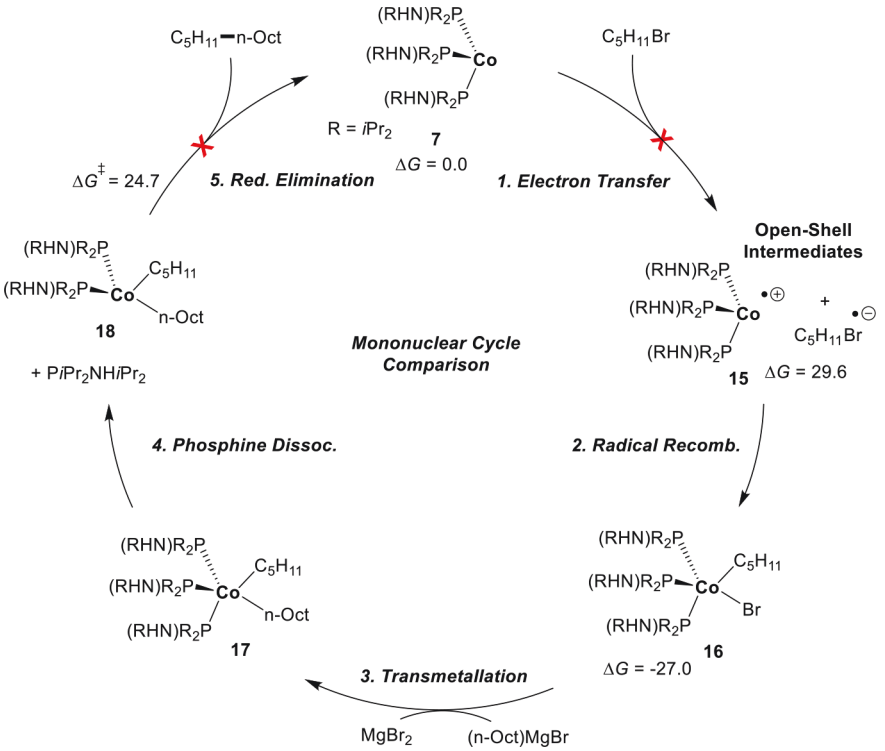

[a]Values in kilocalories per mole.

very slow, turnover-limiting step without phosphine dissociation. The Co−Zr distances suggest that the Co−Zr interaction remains important in **TS14**. In **TS14**, the Co−Zr interaction distance decreases to 2.50 Å from 2.65 Å in **14**. After **TS14**, it is thermodynamically favorable for the phosphorus of the phosphinoamide ligand to coordinate to the Co metal center to regenerate catalyst **5**.

With the identification of reductive elimination occurring through a phosphine dissociation pathway, we now propose a complete catalytic cycle for catalyst **5** (Scheme 4c), which demonstrates the importance of the synergistic Co and Zr metal centers and phosphinoamide ligands. As discussed previously, the Co−Zr interaction, assembled by a phosphinoamide ligand, provides a thermodynamically feasible pathway for two-electron reduction of precatalyst **1** to **5**. The high electron donor capacity of **5** provides fast outer-sphere ET in step 1. The resulting open-shell intermediates can undergo radical combination in step 2 to give oxidative addition intermediate **8**. Step 3 involves thermodynamically viable *n*-Oct group transfer from the Grignard reagent to the Co metal center that results in dialkyl intermediate **12**. Step 4 involves dissociation of phosphine from the Co metal center, which enables a low-barrier reductive elimination in step 5. This showcases the importance of the phosphinoamide ligands where the amido group directs the Zr metal center while providing a labile phosphine to coordinate to Co. Because of the low-energy phosphine dissociation reductive elimination pathway, transmetalation with a relatively high thermodynamic reaction energy is likely turnover-limiting. While Zr enables very fast Co-centered catalytic reaction steps, it is likely that similar Lewis acidic early transition metals could also serve the same role.

Comparison to Mononuclear Complexes. Direct comparison of dinuclear versus mononuclear catalysis is often difficult because mononuclear analogues generally have different ligands and oxidation states. The mononuclear analogue $ICo(Ph_2PNHiPr)_3$ **6** has the same Co oxidation state as and phosphinoamine ligands very similar to those of dinuclear precatalyst **1**. This mononuclear complex did not provide efficient catalysis and gave only trace yields. To make the most direct comparison to proposed dinuclear catalyst **5**, especially for the key reductive elimination step, we examined the one-electron-reduced complex $Co(iPr_2PNHiPr)_3$ **7** as well as the corresponding two-electron-reduced complex $[Co(iPr_2PNHiPr)_3]^-$. We also considered the possibility that **6** is activated to $Co(iPr_2PNHiPr)_3(n\text{-Oct})$ by reaction with $[(n\text{-Oct})MgBr]_2$ (see the Supporting Information).

The oxidative addition between **7** and 1-bromopentane to give the corresponding $(iPr_2PNHiPr)_3Co(C_5H_{11})(Br)$ complex **16** is exergonic by 27.0 kcal/mol (Scheme 5). This thermodynamically favorable reaction contrasts with the endergonic oxidative addition between **5** and 1-bromopentane. While this mononuclear oxidative addition is thermodynamically viable, ET to begin the oxidative addition is endergonic. ET from **7** to 1-bromopentane to give $[Co(iPrNPiPr_2)_3]^+$ (**15**), $(C_5H_{11})^*$, and Br^- is endergonic by 29.6 kcal/mol. This >18 kcal/mol larger ET energy for the mononuclear Co complex versus that of the Co−Zr complex is consistent with the HOMO orbital of **7** being ∼0.5 eV lower in energy than the HOMO of **5**. The difference in ET capacity is that **7** is a one-electron-reduced complex while **5** is a two-electron-reduced complex.

Transmetalation between **16** and $[(n\text{-Oct})MgBr]_2$ provides the dialkyl intermediate $(iPr_2PNHiPr)_3Co(C_5H_{11})(n\text{-Oct})$ **17** with a <1 kcal/mol energy change. From **17**, there is a three-center reductive elimination transition-state structure that is very similar to **TS12**. The $\Delta G^{\ddagger}$ for this mononuclear reductive elimination is 26.9 kcal/mol, which is ∼14 kcal/mol lower in

DOI: 10.1021/acs.organomet.8b00449
Organometallics 2018, 37, 4195−4203

energy than dinuclear transition state **TS12**. More importantly, the low-energy phosphine dissociation/reductive elimination dinuclear pathway is not available for this mononuclear complex. For **17**, phosphine dissociation lowers the reductive elimination to only 24.7 kcal/mol (a 2.2 kcal/mol decrease). Importantly, the energies for both ET and reductive elimination for this mononuclear Co analogue showcase the multiple advantages of the Co−Zr interaction for fast catalysis.

We also examined the possible anionic mononuclear complex $[Co(iPr_2PNHiPr)_3]^-$. As expected, this two-electron-reduced species is significantly better at ET than **7**. For $[Co(iPr_2PNHiPr)_3]^-$ ET to 1-bromopentane, ΔG = −10.5 kcal/mol to generate $Co(iPrNHPiPr_2)_3$, (C_5H_{11})*, and Br^-. The overall oxidative addition to give $[(iPrNHPiPr_2)_3Co(C_5H_{11})(Br)]^-$ is exergonic by 28.5 kcal/mol. Grignard-facilitated transmetalation to give $[(iPrNHPiPr_2)_3Co(C_5H_{11})(n\text{-Oct})]^-$ requires only 9.0 kcal/mol (ΔG = −21.2 kcal/mol). Similar to that of dialkyl dinuclear intermediate **12**, phosphine dissociation at this electron rich structure is favorable, by 3.9 kcal/mol. However, while ET/oxidative addition and transmetalation are potentially better for the mononuclear model than for dinuclear **5**, because there is no Zr metal center, reductive elimination from $[(iPrNHPiPr_2)_2Co(C_5H_{11})(Oct)]^-$ has a large barrier ($\Delta G^{\ddagger}$) of 24.1 kcal/mol.

CONCLUSIONS

The metal−metal interaction in the heterodinuclear Co−Zr catalyst promotes fast Kumada coupling catalysis between alkyl halide and Grignard components for several reasons. (1) The electron withdrawing capacity through a direct Co−Zr interaction provides a viable route to a two-electron-reduced active catalyst **5** from the starting precatalyst **1**. (2) This two-electron-reduced intermediate **5** promotes low-energy ET to induce oxidative addition. (3) The electron withdrawing capacity of the Zr metal, and the phosphinoamide ligands bridging Co and Zr metal centers, provides a low-energy reductive elimination route through an intramolecular phosphine dissociation pathway. Comparison to analogous one-electron- and two-electron-reduced mononuclear Co complexes reveals that there is no low-energy phosphine dissociation/reductive elimination route possible.

COMPUTATIONAL DETAILS

All ground-state and transition-state geometries were optimized in Gaussian 09[27] using the restricted and unrestricted M06-L[28] functional with an ultrafine integration grid. The 6-31G(d,p) basis set was used for H, C, N, O, Mg, and Cl. The LANL2DZ[29] pseudopotential/basis set was used for Co, Br, Zr, and I. Geometries were confirmed as minima or transition-state structures by normal-mode vibrational frequency analysis. Conformational analysis and evaluation of multiple spin states were performed for all ground states and transition states. Intrinsic reaction coordinate (IRC) calculations were used to verify the connection between transition states and intermediates. Electronic energies were calculated with the def2-TZVP basis set.[30] Reported free energies correspond to (U)M06-L/def2-TZVP//(U)M06-L/6-31G(d,p)[LANL2DZ for Co, Br, Zr, and I]. The continuum SMD[31] THF model was used for all optimization and single-point energy evaluations. The Grignard species was approximated as a dinuclear-bridged $[(n\text{-Oct})MgBr]_2$ structure. The resulting inorganic Mg salts were treated as molecular rather than complex solids.

ASSOCIATED CONTENT

Supporting Information

The Supporting Information is available free of charge on the ACS Publications website at DOI: 10.1021/acs.organomet.8b00449.

Energies and more computational details (PDF)

xyz coordinates (XYZ)

AUTHOR INFORMATION

Corresponding Author

*E-mail: dhe@chem.byu.edu.

ORCID

Christine M. Thomas: 0000-0001-5009-0479

Daniel H. Ess: 0000-0001-5689-9762

Notes

The authors declare no competing financial interest.

ACKNOWLEDGMENTS

D.H.E. thanks Brigham Young University (BYU) and the Fulton Supercomputing Lab (FSL). This work was supported by the National Science Foundation Chemical Catalysis Program (CHE-1764194, to D.H.E.). J.C. and D.P. thank the BYU Department of Chemistry and Biochemistry and College of Physical and Mathematical Sciences for undergraduate research awards. D.-H.K. thanks the BYU College of Physical and Mathematical Sciences for a fellowship. C.M.T. acknowledges support by the U.S. Department of Energy, Office of Science, Office of Basic Energy Sciences, Chemical Sciences, Geosciences, and Biosciences Division, under Award DE-SC0014151.

REFERENCES

(1) (a) Sinfelt, J. H. *Bimetallic Catalysts: Discoveries, Concepts and Applications*; John Wiley and Sons: New York, 1983. (b) Bullock, R. M.; Casey, C. P. Heterobimetallic Compounds Linked by Heterodifunctional Ligands. *Acc. Chem. Res.* **1987**, *20*, 167−173. (c) Zanello, P.; Tamburini, S.; Vigato, P. A.; Mazzocchin, G. A. Synthesis, Structure and Electrochemical Characterization of Homo- and Heterodinuclear Copper Complexes with Compartmental Ligands. *Coord. Chem. Rev.* **1987**, *77*, 165−273. (d) Stephan, D. W. Early-late Heterobimetallics. *Coord. Chem. Rev.* **1989**, *95*, 41−107. (e) van den Beuken, E. K.; Feringa, B. L. Bimetallic Catalysis by Late Transition Metal Complexes. *Tetrahedron* **1998**, *54*, 12985−13011. (f) Wheatley, N.; Kalck, P. Structure and Reactivity of Early-Late Heterobimetallic Complexes. *Chem. Rev.* **1999**, *99*, 3379−3419. (g) Gade, L. H. Highly Polar Metal-Metal Bonds in "Early-Late" Heterobimetallic Complexes. *Angew. Chem., Int. Ed.* **2000**, *39*, 2658−2678. (h) Oro, L. A.; Sola, E. Mechanistic Aspects of Dihydrogen Activation and Catalysis by Dinuclear Complexes. In *Recent Advances in Hydride Chemistry*; Elsevier, 2001; pp 299−327.

(2) (a) Hostetler, M. J.; Bergman, R. G. Synthesis and Reactivity of Cp Synthesis and Reactivity of $Cp_2Ta(CH_2)_2Ir(CO)_2$ an Early-late Heterobimetallic Complex that Catalytically Hydrogenates, Isomerizes and Hydrosilates Alkenes. *J. Am. Chem. Soc.* **1990**, *112*, 8621−8623. (b) Hostetler, M. J.; Butts, M. D.; Bergman, R. G. Scope and Mechanism of Alkene Hydrogenation/Isomerization Catalyzed by Complexes of the type $R_2E(CH_2)_2M(CO)(L)$ (R = Cp, Me, Ph; E = Phosphorus, Tantalum; M = Rhodium, Iridium; L = CO, PPh_3). *J. Am. Chem. Soc.* **1993**, *115*, 2743−2752. (c) Hostetler, M. J.; Butts, M. D.; Bergman, R. G. Rate and Equilibrium Study of the Reversible Oxidative Addition of Silanes to the Iridium Center in $Cp_2Ta(\mu\text{-}CH_2)_2Ir(CO)_2$ and of Alkene Hydrosilation/Isomerization Catalyzed by This System. *Organometallics* **1993**, *12*, 65−75.

DOI: 10.1021/acs.organomet.8b00449
Organometallics 2018, 37, 4195−4203

(3) (a) Gelmini, L.; Stephan, D. W. Preparation, Reactivity, Hydroformylation Catalysis, and Structural Studies of the Early Transition Metal/Late Transition Metal Heterobimetallic Complexes $Cp_2M(\mu\text{-}PR_2)_2M'H(CO)PPh_3$ (M = Zr, Hf; M' = Rh, Ir). *Organometallics* **1988**, *7*, 849−855. (b) Rida, M. A.; Smith, A. K. A Bimetallic Hydroformylation Catalyst: High Regioselectivity through Heterobimetallic Cooperativity. *J. Mol. Catal. A: Chem.* **2003**, *202*, 87−95. (c) Dickson, R. S.; De Simone, T.; Campi, E. M.; Jackson, W. R. Hydroformylation of Alkenes and Alkynes using a Heterobinuclear Rh-W Catalyst. *Inorg. Chim. Acta* **1994**, *220*, 187−192.

(4) (a) Lindenberg, F.; Shribman, T.; Sieler, J.; Hey-Hawkins, E.; Eisen, M. Dinuclear Phosphido- and Arsenido Early/Late Transition Metal Complexes. Efficient Catalysts for Ethylene Polymerization. *J. Organomet. Chem.* **1996**, *515*, 19−25. (b) Motta, A.; Fragalà, I. L.; Marks, T. J. Proximity and Cooperativity Effects in Binuclear d Olefin Polymerization Catalysis. Theoretical Analysis of Structure and Reaction Mechanism. *J. Am. Chem. Soc.* **2009**, *131*, 3974−3984. (c) Yan, X.; Chernega, A.; Green, M. L. H.; Sanders, J.; Souter, J.; Ushioda, T. Homo- and Hetero-binuclear Ansa-metallocenes of the Group 4 Transition Metals as Homogeneous Co-catalysts for the Polymerization of Ethane and Propene. *J. Mol. Catal. A: Chem.* **1998**, *128*, 119−141.

(5) (a) Ozawa, F.; Park, J. W.; Mackenzie, P. B.; Schaefer, W. P.; Henling, L. M.; Grubbs, R. H. Structure and Reactivity of Titanium-Platinum and -Palladium Heterobinuclear Complexes μ-Methylene Ligands. *J. Am. Chem. Soc.* **1989**, *111*, 1319−1327. (b) Dias, E. L.; Grubbs, R. H. Synthesis and Investigation of Homo- and Heterobimetallic Ruthenium Olefin Metathesis Catalysts Exhibiting Increased Activities. *Organometallics* **1998**, *17*, 2758−2767.

(6) (a) Thomas, C. M. Metal-metal Multiple Bonds in Early/Late Heterobimetallic Complexes: Applications Toward Small Molecule Activation and Catalysis. *Comments Inorg. Chem.* **2011**, *32*, 14. (b) Cooper, B. G.; Napoline, J. W.; Thomas, C. M. Catalytic Applications of Early/Late Heterobimetallic Complexes. *Catal. Rev.: Sci. Eng.* **2012**, *54*, 1−40.

(7) (a) Mankad, N. P. Selectivity Effects in Bimetallic Catalysis. *Chem. - Eur. J.* **2016**, *22*, 5822−5829. (b) Powers, I. G.; Uyeda, C. Metal-Metal Bonds in Catalysis. *ACS Catal.* **2017**, *7*, 936−958. (c) Pye, D. R.; Mankad, N. P. Bimetallic catalysis for C-C and C-X coupling reactions. *Chem. Sci.* **2017**, *8*, 1705−1718.

(8) (a) Powers, D. C.; Ritter, T. Bimetallic Redox Synergy in Oxidative Palladium Catalysis. *Acc. Chem. Res.* **2012**, *45*, 840−850. (b) Kornecki, K. P.; Berry, J. F.; Powers, D. C.; Ritter, T. Metal-Metal Bond-Containing Complexes as Catalysts for C-H Functionalization. *Prog. Inorg. Chem.* **2014**, *58*, 225−302. (c) Berry, J. F. Metal-Metal Multiple Bonded Intermediates in Catalysis. *J. Chem. Sci.* **2015**, *127*, 209−214. (d) Blakemore, J. D.; Crabtree, R. H.; Brudvig, G. W. Molecular Catalysts for Water Oxidation. *Chem. Rev.* **2015**, *115*, 12974−13005. (e) Eisenhart, R. J.; Clouston, L. J.; Lu, C. C. Configuring Bonds Between First-Row Transition Metals. *Acc. Chem. Res.* **2015**, *48*, 2885−2894. (f) Buchwalter, P.; Rose, J.; Braunstein, P. Multimetallic Catalysis Based on Heterometallic Complexes and Clusters. *Chem. Rev.* **2015**, *115*, 28−126. (g) Kalck, P., Ed. *Homo- and Heterobimetallic Complexes in Catalysis: Cooperative Catalysis Topics in Organometallic Chemistry*; Springer, 2016; Vol. *59*. (h) Ritleng, V.; Chetcuti, M. J. Hydrocarbyl Ligand Transformations on Heterobimetallic Complexes. *Chem. Rev.* **2007**, *107*, 797−858. (i) Maggini, S. Classification of P,N-binucleating Ligands for Hetero- and Homobimetallic Complexes. *Coord. Chem. Rev.* **2009**, *253*, 1793−1832. (j) van der Vlugt, J. I. van der Cooperative Catalysis with First-Row Late Transition Metals. *Eur. J. Inorg. Chem.* **2012**, *2012*, 363−375. (k) Bratko, I.; Gómez, M. Polymetallic complexes linked to a single-frame ligand: cooperative effects in catalysis. *Dalton Trans.* **2013**, *42*, 10664−10681.

(9) Mazzacano, T. J.; Mankad, N. P. Base Metal Catalysts for Photochemical C-H Borylation that Utilize Metal-Metal Cooperativity. *J. Am. Chem. Soc.* **2013**, *135*, 17258−17261.

(10) Cammarota, R. C.; Vollmer, M. V.; Xie, J.; Ye, J.; Linehan, J. C.; Burgess, S. A.; Appel, A. M.; Gagliardi, L.; Lu, C. C. A bimetallic Nickel-Gallium Complex Catalyzes CO_2 Hydrogenation via the Intermediacy of an Anionic d^{10} Nickel Hydride. *J. Am. Chem. Soc.* **2017**, *139*, 14244−14250.

(11) Siedschlag, R. B.; Bernales, V.; Vogiatzis, K. D.; Planas, N.; Clouston, L. J.; Bill, E.; Gagliardi, L.; Lu, C. C. Catalytic Silylation of Dinitrogen with a Dicobalt Complex. *J. Am. Chem. Soc.* **2015**, *137*, 4638−4641.

(12) (a) Parmelee, S. R.; Mazzacano, T. J.; Zhu, Y.; Mankad, N. P.; Keith, J. A. A Heterobimetallic Mechanism for C-H Borylation Elucidated from Experimental and Computational Data. *ACS Catal.* **2015**, *5*, 3689−3699. (b) Luo, G.; Luo, Y.; Hou, Z.; Qu, J. Intermetallic Cooperation in Olefin Polymerization Catalyzed by a Binuclear Samarocene Hydride: A Theoretical Study. *Organometallics* **2016**, *35*, 778−784. (c) Bernales, V.; League, A. B.; Li, Z.; Schweitzer, N. M.; Peters, A. W.; Carlson, R. K.; Hupp, J. T.; Cramer, C. J.; Farha, O. K.; Gagliardi, L. Computationally Guided Discovery of a Catalytic Cobalt-Decorated Metal-Organic Framework for Ethylene Dimerization. *J. Phys. Chem. C* **2016**, *120*, 23576−23583.

(13) Walker, W. K.; Kay, B. M.; Michaelis, S. A.; Anderson, D. L.; Smith, S. J.; Ess, D. H.; Michaelis, D. J. Origin of Fast Catalysis in Allylic Amination Reactions Catalyzed by Pd-Ti Heterobimetallic Complexes. *J. Am. Chem. Soc.* **2015**, *137*, 7371−7378.

(14) Zhang, Y.; Roberts, S. P.; Bergman, R. G.; Ess, D. H. Mechanism and Catalytic Impact of Ir-Ta Heterobimetallic and Ir-P Transition Metal/Main Group Interactions on Alkene Hydrogenation. *ACS Catal.* **2015**, *5*, 1840−1849.

(15) Zhou, W.; Napoline, J. W.; Thomas, C. M. A Catalytic Application of Co/Zr Heterobimetallic Complexes: Kumada Coupling of Unactivated Alkyl Halides with Alkyl Grignard Reagents. *Eur. J. Inorg. Chem.* **2011**, *2011*, 2029−2033.

(16) (a) Greenwood, B. P.; Forman, S. I.; Rowe, G. T.; Chen, C.-H.; Foxman, B. M.; Thomas, C. M. Multielectron Redox Activity Facilitated by Metal-Metal Interactions in Early/Late Heterobimetallics: Co/Zr Complexes Supported by Phosphinoamide Ligands. *Inorg. Chem.* **2009**, *48*, 6251−6260. (b) Greenwood, B. P.; Rowe, G. T.; Chen, C.-H.; Foxman, B. M.; Thomas, C. M. Metal-Metal Multiple Bonds in Early/Late Heterobimetallics Support Unusual Trigonal Monopyramidal Geometries at both Zr and Co. *J. Am. Chem. Soc.* **2010**, *132*, 44−45. (c) Thomas, C. M.; Napoline, J. W.; Rowe, G. T.; Foxman, B. M. Oxidative Addition across Zr/Co Multiple Bonds in Early/Late Heterobimetallic Complexes. *Chem. Commun.* **2010**, *46*, 5790−5792. (d) Setty, V. N.; Zhou, W.; Foxman, B. M.; Thomas, C. M. Subtle Differences Between Zr and Hf in Early/Late Heterobimetallic Complexes with Cobalt. *Inorg. Chem.* **2011**, *50*, 4647−4655. (e) Krogman, J. P.; Foxman, B. M.; Thomas, C. M. Activation of CO_2 by a Heterobimetallic Zr/Co Complex. *J. Am. Chem. Soc.* **2011**, *133*, 14582−14585. (f) Evers, D. A.; Bluestein, A. H.; Foxman, B. M.; Thomas, C. M. Synthesis and Investigation of the Metal-Metal Interactions in Early/Late Heterobimetallic Complexes Linking Group 5 Imido Fragments to Co(I). *Dalton Transactions* **2012**, *41*, 8111−8115. (g) Napoline, J. W.; Bezpalko, M. W.; Foxman, B. M.; Thomas, C. M. N-H Activation of Hydrazines by a Heterobimetallic Zr-Co Complex: Promotion of One-electron Chemistry at Zr. *Chem. Commun.* **2013**, *49*, 4388−4390. (h) Mathialagan, R.; Kuppuswamy, S.; De Denko, A. T.; Bezpalko, M. W.; Foxman, B. M.; Thomas, C. M. Metal-Metal Bonding in Low-Coordinate Dicobalt Complexes Supported by Phosphinoamide Ligands. *Inorg. Chem.* **2013**, *52*, 701−706. (i) Zhou, W.; Marquard, S. L.; Bezpalko, M. W.; Foxman, B. M.; Thomas, C. M. Catalytic Hydrosilylation of Ketones Using a Co/Zr Heterobimetallic Complex: Evidence for an Unusual Mechanism Involving Ketyl Radicals. *Organometallics* **2013**, *32*, 1766−1772. (j) Krogman, J. P.; Bezpalko, M. W.; Foxman, B. M.; Thomas, C. M. Synthesis, Structure, and Reactivity of an Anionic Zr-Oxo Relevant to CO_2 Reduction by a Zr/Co Heterobimetallic Complex. *Inorg. Chem.* **2013**, *52*, 3022−3031. (k) Napoline, J. W.; Krogman, J. P.; Shi, R.; Kuppuswamy, S.; Bezpalko, M. W.; Foxman, B. M.; Thomas, C. M. Activation of E-H and E-E (E = S, O) Bonds by Heterobimetallic Zr/Co Complexes: Evidence for Both One- and Two-Electron Processes. *Eur. J. Inorg. Chem.* **2013**, *2013*, 3874−3882. (l) Krogman, J. P.; Thomas, C. M. Metal-Metal Multiple Bonding in C_3-symmetric Bimetallic

DOI: 10.1021/acs.organomet.8b00449
Organometallics 2018, 37, 4195−4203

Complexes of the First Row Transition Metals. *Chem. Commun.* **2014**, *50*, 5115−5127. (m) Marquard, S. L.; Bezpalko, M. W.; Foxman, B. M.; Thomas, C. M. Interaction and Activation of Carbon-heteroatom π bonds with a Zr/Co Heterobimetallic Complex. *Organometallics* **2014**, *33*, 2071−2079. (n) Krogman, J. P.; Gallagher, J. R.; Zhang, G.; Hock, A. S.; Miller, J. T.; Thomas, C. M. Assignment of the Oxidation States of Zr and Co in a Highly Reactive Heterobimetallic Zr/Co Complex Using X-ray Absorption Spectroscopy (XANES). *Dalton Trans.* **2014**, *43*, 13852−13857. (o) Wu, B.; Hernandez Sanchez, R.; Bezpalko, M. W.; Foxman, B. M.; Thomas, C. M. Formation of Heterobimetallic Zirconium/Cobalt Diimido Complexes via a Four-Electron Transformation. *Inorg. Chem.* **2014**, *53*, 10021−10023. (p) Saper, N. I.; Bezpalko, M. W.; Foxman, B. M.; Thomas, C. M. Synthesis of Chiral Heterobimetallic Tris(phosphinoamide) Zr/Co Complexes. *Polyhedron* **2016**, *114*, 88−95. (q) Zhang, H.; Wu, B.; Marquard, S. L.; Litle, E. D.; Dickie, D. A.; Bezpalko, M. W.; Foxman, B. M.; Thomas, C. M. Investigation of Ketone C = O Bond Activation Processes by Heterobimetallic Zr/Co and Ti/Co Tris(phosphinoamide) Complexes. *Organometallics* **2017**, *36*, 3498−3507.

(17) (a) Cahiez, G.; Moyeux, A. Cobalt-Catalyzed Cross-Coupling Reactions. *Chem. Rev.* **2010**, *110*, 1435−1462. (b) Knochel, P.; Thaler, T.; Diene, C. Pd-, Ni-, Fe-, and Co-Catalyzed Cross-Coupling Using Functionalized Zn-, Mg-, Fe-, and In-Organometallics. *Isr. J. Chem.* **2010**, *50*, 547−557. (c) Knappke, C. E. I.; Jacobi von Wangelin, A. 35 Years of Palladium-catalyzed Cross-coupling with Grignard Reagents: How Far Have We Come? *Chem. Soc. Rev.* **2011**, *40*, 4948−4962.

(18) (a) Iwasaki, T.; Kambe, N. Coupling Reactions Between sp^3-Carbon Centers. *Comprehensive Organic Synthesis*, 2nd ed.; 2014; Vol. 3, pp 337−391. (b) Iwasaki, T.; Takagawa, H.; Okamoto, K.; Singh, S. P.; Kuniyasu, H.; Kambe, N. The Cobalt-Catalyzed Cross-Coupling Reaction of Alkyl Halides with Alkyl Grignard Reagents: A New Route to Constructing Quaternary Carbon Centers. *Synthesis* **2014**, *46*, 1583−1592. (c) Iwasaki, T.; Takagawa, H.; Singh, S. P.; Kuniyasu, H.; Kambe, N. Co-Catalyzed Cross-Coupling of Alkyl Halides with Teriary Alkyl Grignard Reagents Using a 1,3-Butadiene Additive. *J. Am. Chem. Soc.* **2013**, *135*, 9604−9607. (d) Cahiez, G.; Chaboche, C.; Duplais, C.; Giulliani, A.; Moyeux, A. Cobalt-Catalyzed Cross-Coupling Reaction between Functionalized Primary and Secondary Alkyl Halides and Aliphatic Grignard Reagents. *Adv. Synth. Catal.* **2008**, *350*, 1484−1488.

(19) (a) Gao, H.; Zhou, Z.; Kwon, D.-H.; Coombs, J.; Jones, S.; Behnke, N. E.; Ess, D. H.; Kürti, L. Rapid Heteroatom Transfer to Arylmetals Utilizing Multifunctional Reagent Scaffolds. *Nat. Chem.* **2016**, *9*, 681−688. (b) Kattamuri, P. V.; Yin, J.; Siriwongsup, S.; Kwon, D.-H.; Ess, D. H.; Li, Q.; Li, G.; Yousufuddin, M.; Richardson, P. F.; Sutton, S. C.; Kürti, L. Practical Singly and Doubly Electrophillic Aminating Agents: A New, More Sustainable Platform for Carbon-Nitrogen Bond Formation. *J. Am. Chem. Soc.* **2017**, *139*, 11184−11196.

(20) Terao, J.; Kambe, N. Cross-Coupling Reaction of Alkyl Halides with Grignard Reagents Catalyzed by Ni, Pd, or Cu Complexes with π-Carbon Ligand(s). *Acc. Chem. Res.* **2008**, *41*, 1545−1554.

(21) (a) Tsuji, T.; Yorimitsu, H.; Oshima, K. Cobalt-Catalyzed Coupling Reaction of Alkyl Halides with Allylic Grignard Reagents. *Angew. Chem.* **2002**, *114*, 4311−4313. (b) Ohmiya, H.; Tsuji, T.; Yorimitsu, H.; Oshima, K. Cobalt-Catalyzed Cross-Coupling Reactions of Alkyl Halides with Allylic and Benzylic Grignard Reagents and Their Application to Tandem Radical Cyclization/Cross-Coupling Reactions. *Chem. - Eur. J.* **2004**, *10*, 5640−5648. (c) Affo, W.; Ohmiya, H.; Fujioka, T.; Ikeda, Y.; Nakamura, T.; Yorimitsu, H.; Oshima, K.; Imamura, Y.; Mizuta, T.; Miyoshi, K. Cobalt-Catalyzed Trimethylsilylmethylmagnesium-Promoted Radical Alkenylation of Alkyl Halides: A Complement to the Heck Reaction. *J. Am. Chem. Soc.* **2006**, *128*, 8068−8077. (d) Despiau, C. F.; Dominey, A. P.; Harrowven, D. C.; Linclau, B. Total Synthesis of (±)-Paroxetine by Diastereoconvergent Cobalt-Catalysed Arylation. *Eur. J. Org. Chem.* **2014**, *2014*, 4335−4341. (e) Gonnard, L.; Guérinot, A.; Cossy, J. Cobalt-Catalyzed Cross-Coupling of 3- and 4-Iodopiperidines with Grignard Reagents. *Chem. - Eur. J.* **2015**, *21*, 12797−12803. (f) Guo, X.-K.; Zhang, L.-B.; Wei, D.; Niu, J.-L. Mechanistic insights into cobalt(II/III)-catalyzed C-H oxidation: a combined theoretical and experimental study. *Chem. Sci.* **2015**, *6*, 7059−7071. (g) Whiteoak, C. J.; Planas, O.; Company, A.; Ribas, X. A First Example of Cobalt-Catalyzed Remote C-H Functionalization of 8-Aminoquinolines Operating through a Single Electron Transfer Mechanism. *Adv. Synth. Catal.* **2016**, *358*, 1679−1688.

(22) Ahmad, K.; Chang, C.-R.; Li, J. Mechanistic investigations of Co(II)-Catalyzed C-N coupling reactions. *J. Organomet. Chem.* **2018**, *868*, 144−153.

(23) (a) Tsou, T. T.; Kochi, J. K. Mechanism of Oxidative Addition. Reaction of Nickel(0) Complexes with Aromatic Halides. *J. Am. Chem. Soc.* **1979**, *101*, 6319−6332. (b) Morrell, D. G.; Kochi, J. K. Mechanistic Studies of Nickel Catalysis in the Cross Coupling of Aryl Halides with Alkylmetals. Role of ArylalkylNickel(II) Species as Intermediates. *J. Am. Chem. Soc.* **1975**, *97*, 7262−7270.

(24) (a) Bauer, G.; Wodrich, M. D.; Scopelliti, R.; Hu, X. Iron Pincer Complexes as Catalysts and Intermediates in Alkyl-Aryl Kumada Coupling Reactions. *Organometallics* **2015**, *34*, 289−298. (b) Breitenfeld, J.; Wodrich, M. D.; Hu, X. Bimetallic Oxidative Addition in Nickel-Catalyzed Alkyl-Aryl Kumada Coupling Reactions. *Organometallics* **2014**, *33*, 5708−5715.

(25) Daifuku, S. L.; Al-Afyouni, M. H.; Snyder, B. E. R.; Kneebone, J. L.; Neidig, M. L. A Combined Mossbauer, Magnetic Circular Dichroism, and Density Functional Theory Approach for Iron Cross-Coupling Catalysis: Electronic Structure, In Situ Formation, and Reactivity of Iron-Mesityl-Bisphosphines. *J. Am. Chem. Soc.* **2014**, *136*, 9132−9143.

(26) Xu, H.; Bernskoetter, W. H. Mechanistic Considerations for C-C Bond Reductive Coupling at a Cobalt(III) Center. *J. Am. Chem. Soc.* **2011**, *133*, 14956−14959.

(27) Frisch, M. J.; Trucks, G. W.; Schlegel, H. B.; Scuseria, G. E.; Robb, M. A.; Cheeseman, J. R.; Scalmani, G.; Barone, V.; Mennucci, B.; Petersson, G. A.; Nakatsuji, H.; Caricato, M.; Li, X.; Hratchian, H. P.; Izmaylov, A. F.; Bloino, J.; Zheng, G.; Sonnenberg, J. L.; Hada, M.; Ehara, M.; Toyota, K.; Fukuda, R.; Hasegawa, J.; Ishida, M.; Nakajima, T.; Honda, Y.; Kitao, O.; Nakai, H.; Vreven, T.; Montgomery, J. A., Jr.; Peralta, J. E.; Ogliaro, F.; Bearpark, M.; Heyd, J. J.; Brothers, E.; Kudin, K. N.; Staroverov, V. N.; Kobayashi, R.; Normand, J.; Raghavachari, K.; Rendell, A.; Burant, J. C.; Iyengar, S. S.; Tomasi, J.; Cossi, M.; Rega, N.; Millam, J. M.; Klene, M.; Knox, J. E.; Cross, J. B.; Bakken, V.; Adamo, C.; Jaramillo, J.; Gomperts, R.; Stratmann, R. E.; Yazyev, O.; Austin, A. J.; Cammi, R.; Pomelli, C.; Ochterski, J. W.; Martin, R. L.; Morokuma, K.; Zakrzewski, V. G.; Voth, G. A.; Salvador, P.; Dannenberg, J. J.; Dapprich, S.; Daniels, A. D.; Farkas; Foresman, J. B.; Ortiz, J. V.; Cioslowski, J.; Fox, D. J. *Gaussian 09*, revision B.01; Gaussian, Inc.: Wallingford, CT, 2009.

(28) (a) Zhao, Y.; Truhlar, D. G. A New Local Density Functional for Main-Group Thermochemistry, Transition Metal Bonding, Thermochemical Kinetics, and Noncovalent Interactions. *J. Chem. Phys.* **2006**, *125*, 194101. (b) Zhao, Y.; Truhlar, D. The M06 Suite of Density Functionals for Main Group Thermochemistry, Thermochemical Kinetics, Noncovalents Interactions, Excited States, and Transition Elements: Two New Functionals and Systematic Testing of Four M06-class Functionals and 12 other functionals. *Theor. Chem. Acc.* **2008**, *120*, 215−241. (c) Zhao, Y.; Truhlar, D. G. Density Functionals with Broad Applicability in Chemistry. *Acc. Chem. Res.* **2008**, *41*, 157−167.

(29) Wadt, W. R.; Hay, P. J. Ab Initio Effective Core Potentials for Molecular Calculations. Potentials for Main Group Elements Sodium to Bismuth. *J. Chem. Phys.* **1985**, *82*, 284−298.

(30) (a) Def2-TZVP basis sets were downloaded from https://bse.pnl.gov/bse/portal (accessed January 1, 2016). (b) Weigend, F.; Ahlrichs, R. *Phys. Chem. Chem. Phys.* **2005**, *7*, 3297−3305.

(31) Marenich, A. V.; Cramer, C. J.; Truhlar, D. G. Universal Solvation Model Based on Solute Electron Density and on a Continuum Model of the Solvent Defined by the Bulk Dielectric Constant and Atomic Surface Tensions. *J. Phys. Chem. B* **2009**, *113*, 6378−6396.

DOI: 10.1021/acs.organomet.8b00449
Organometallics 2018, 37, 4195−4203